HHS Public Access

Author manuscript

Oncogene. Author manuscript; available in PMC 2023 May 24.

Published in final edited form as:

Oncogene. 2023 May ; 42(21): 1716–1727. doi:10.1038/s41388-023-02688-5.

RON-augmented cholesterol biosynthesis in breast cancer metastatic progression and recurrence

Brian G Hunt[1], **James C Davis**[1], **Levi H Fox**[1], **Sara Vicente-Muñoz**[2,3], **Carissa Lester**[1], **Susanne I Wells**[3,4], **Susan E Waltz**[*,1,5]

[1]Department of Cancer Biology, University of Cincinnati College of Medicine, Cincinnati, OH 45267-0521, USA

[2]Division of Pathology, NMR-Metabolomics Core, Cincinnati Children's Hospital Medical Center, OH 45229-3026, USA

[3]Department of Pediatrics, University of Cincinnati College of Medicine, Cincinnati, OH 45229-3026, USA

[4]Division of Oncology, Cincinnati Children's Hospital Medical Center, Cincinnati, OH 45229, USA

[5]Research Service, Cincinnati Veterans Affairs Hospital Medical Center, Cincinnati, OH 45220, USA

Abstract

Recurrence remains a significant clinical barrier to improving breast cancer patient outcomes. The RON receptor is a predictor of metastatic progression and recurrence in breast cancers of all subtypes. RON directed therapies are in development, but pre-clinical data directly testing the impact of RON inhibition on metastatic progression/recurrence are lacking, and mechanisms to exert this function remain unclear. Herein, we modeled breast cancer recurrence using implantation of RON-overexpressing murine breast cancer cells. Recurrent growth was examined after tumor resection via *in vivo* imaging and *ex vivo* culture of circulating tumor cells from whole blood samples from tumor bearing mice. *In vitro* functional assessment of was performed using mammosphere formation assays. Transcriptomic pathway enrichment identified glycolysis and cholesterol biosynthesis pathways, transcription factor targets, and signaling pathways enriched in RON-overexpressing breast cancer cells. BMS777607, a RON inhibitor, abrogated CTC colony formation tumor cells and tumor recurrence. RON promoted mammosphere formation through upregulated cholesterol production that utilizes glycolysis-derived substrates. In mouse models with RON overexpression, statin-mediated inhibition of cholesterol biosynthesis impeded metastatic progression and recurrence but does not affect the primary tumor. RON upregulates

[*]Corresponding author. susan.waltz@uc.edu Phone: (513)558-8675. Address: Vontz Center, 3125 Eden Ave, Cincinnati, OH 45267-0521.

AUTHOR CONTRIBUTIONS

The authors have made the following declarations about their contributions: Conceived and designed experiments: B.G.H., S.V.M, S.I.W., and S.E.W. Performed experiments: B.G.H., J.C.D., L.H.F., C.L. and S.V.M. Analyzed data: B.G.H., J.C.D., L.H.F., S.V.M., C.L., S.I.W., and S.E.W. Wrote the paper: B.G.H. and S.E.W. All authors have read and agreed to the published version of the manuscript.

COMPETING INTERESTS STATEMENT: The authors declare no competing interests.

glycolysis and cholesterol biosynthesis gene expression by two pathways: MAPK-dependent c-Myc expression and β-catenin-dependent SREBP2 expression.

INTRODUCTION

Significant improvements in breast cancer (BC) outcomes are evident in the nearly 40% reduction in breast cancer mortality since 1980 (1–3). However, the reduction in the mortality rate has slowed to <2% in the past ten years (4) and 44,000+ individuals in the United States are expected to die of breast cancer annually (2). Despite a marked increase in the number of locally-confined (early stage) breast cancer cases, the risk of metastatic progression/recurrence in breast cancer patients has not decreased (and has likely increased) over time (5). Fear of recurrence has defined breast cancer as one of the most over-diagnosed and over-treated diseases (6).

The RON receptor tyrosine kinase is overexpressed in more than half of all human BCs (7) and a strong relationship exists between RON expression and elevated risk of recurrence (8). Recently, we reported RON expression is a predictor of metastatic progression, poor overall survival, and poor relapse-free survival through evaluation of RON gene expression in human breast cancer samples and associated clinical outcomes in publicly available datasets (9). While there are differential recurrence outcomes based on subtype, breast cancer recurrence is observed in all subtypes (10). Thus, we hypothesize that RON signaling supports breast cancer recurrence in all breast cancer subtypes.

Statins are a class of drugs targeting the HMG-CoA Reductase enzyme used in the mevalonate/cholesterol biosynthesis pathways. Statins are heavily used worldwide to treat and prevent progression of heart disease and coronary artery disease through inhibition of cholesterol production, but the role of statins in cancer has remained unclear (11). Preclinical studies have demonstrated an anti-cancer function of statins, particularly lipophilic statins (Atorvastatin, Simvastatin, Lovastatin), in reducing breast cancer metastatic outgrowth, recurrence, and proliferation even in subtypes with poorer prognoses (HER2+ and triple negative) (12–14). Clinical data further support that lipophilic statins reduce breast cancer progression and recurrence with some variability, supporting a need for mechanistic studies that define instances where statins could be most beneficial (11, 14, 15) including upstream mechanisms regulating cholesterol production, as is the focus herein, and downstream mechanisms elucidating how cholesterol might function in promoting breast cancer (reported examples include signaling effects (16) and membrane dynamics regulated by biophysical properties (17)).

In this study, we experimentally examined the functional role of RON signaling in supporting breast cancer recurrence using preclinical models of recurrence/progression. Importantly, we evaluated the efficacy of the RON inhibitor, BMS777607, in our experimental models to extend the translational impact of our work. BMS777607 has completed Phase I clinical trials and has since been reacquired by Bristol-Meyers-Squibb for further clinical testing (18). A growing body of evidence suggests metabolic plasticity in breast cancer supports breast cancer recurrence and metastatic fitness (19, 20). Transcriptomic analyses identify enrichment of glycolysis and cholesterol biosynthesis

(CBS) pathways in RON-overexpressing cells (21, 22) that we confirmed at the expression and metabolite levels. Functionally, we show a requirement for RON-augmented glycolytic flux and CBS in breast cancer stem cell self-renewal. Cholesterol supplementation rescued self-renewal in the presence of glycolysis or CBS inhibition, suggesting that RON-augmented glycolytic flux feeds into the CBS substrate pool to support robust cholesterol production paired with elevated CBS enzyme expression. Given the tumor repopulation property of cancer stem cells, this subpopulation is thought to play a critical role in metastatic progression/recurrence when disseminated (23). *In vivo* treatment with atorvastatin, a CBS inhibitor, showed no effect on primary tumor growth but ablated metastatic progression and recurrence. Finally, RON-overexpressing breast cancer cells upregulate glycolysis enzyme expression through MAPK-dependent c-Myc regulation and CBS enzyme expression through non-canonical β-catenin dependent SREBP2 regulation. These preclinical data suggest statin and other CBS targeting drug treatments may reduce recurrence risk in patients with RON-overexpressing breast cancer and may spark epidemiological studies of breast cancer recurrence in populations with and without long term statin use.

MATERIALS AND METHODS

Cell Lines.

R7 cells and the isogenic CRISPR knockdown of RON (R7 sgRON) were previously described (22, 24, 25). R7 firefly Luciferase, Lung metastasis, Lymph node metastasis, Tumor #1 (RL3T1) cells were generated from three rounds of serial passage of R7 cells through metastasis in syngeneic mice; cells were retrovirally transduction to stably express firefly luciferase (MSCV-IRES-Luciferase; a gift from the laboratory of Jun-Lin Guan). Doxycycline-inducible shRON (TRCN0000023544) clones of RL3T1 cells were generated using the BLOCK-iT Inducible H1 RNAi Entry Vector Kit (Invitrogen). MCF7 and T47D human luminal breast cancer cell lines with isogenic RON modulations have been characterized previously (22, 26–28). Lentiviral transductions were accomplished with pLKO-puro-FLAG-SREBP2 (Addgene #32018), pLKO.1-puro-empty (Addgene #8453) or pLKO-puro-shMyc (TCRN0000054853). Retroviral transductions were accomplished with MSCV-C-Myc-IRES-GFP (Addgene #18770) or MSCV-Neo-GFP/empty (Plasmid 105505). Stable transfections were accomplished with pcDNA3-β-catenin (wild-type; Addgene #16828) or Y654F/Y670F mutagenized β-catenin (29) while transient transfection was accomplished with Ad5-pLPA-CA-MEK1 (gift from the laboratory of Jeff Molkentin). LiCl (Sigma) treatment for β-catenin activation was performed using 10 mM of LiCl in sterile water to the media followed by incubation for four hours (30).

Mice.

Female mice were used in all experiments and all mice were in an FVB/N background. PyMT mice (Jackson Laboratories, Strain #002374) have been previously described (28, 31–33). Mouse genotyping primers are found in Supplemental Table S1. BMS777607 treatment for RON inhibition in mice was performed using 50 mg/kg/day BMS777607 (Selleckchem) via oral gavage (30). Atorvastatin (Selleckchem) treatment was performed via oral gavage at 20 mg/kg/day (34). Orthotopic implantation for recurrence studies utilized 6–8-week-old

mice; mice were anesthetized, a small incision was made to reveal the mammary gland, and 500,000 RL3T1 cells in 50 μL were injected into the gland. Mammary tumors were measured using calipers and tumor volume was calculated as previously described (35). In PyMT mice, tumor volume per mouse was calculated by adding individual calculated tumor volumes together.

All mice were in a FVB background, were maintained under specific pathogen-free conditions, and were treated in accordance with protocols approved by the Institutional Animal Care and Use Committee of the University of Cincinnati. Sample sizes for mice experiments were selected based on published studies. Mice showing abnormal tumor growth against historical kinetics (whereas not plausibly explained by genotype) were excluded and euthanized (examples include very small body size at weaning, microcephaly, etc.). Randomization for PyMT+ mice and RL3T1 injected mice: mice were randomized into Vehicle, BMS777607, or Atorvastatin treatment arms using random number generator. Blinding measures were not considered necessary and not employed.

In vivo imaging.

To monitor breast cancer recurrence *in vivo*, the luciferin/luciferase signal system was employed. Mice were injected intraperitoneally with 2.5 mg D-luciferin (Cat#122799, Perkin-Elmer), and after 5 minutes were anesthetized and imaged using Xenogen IVIS Lumina (Perkin-Elmer). Prior to surgical resection, a 15 second exposure was used to detect luminescent signal of the primary tumors. Following resection, a 5-minute exposure with dark charge-correction was employed in weekly imaging to monitor for recurrence via luminescent signal. At the first sign of recurrent signal detection, a relapse-free survival (RFS) event was recorded. When mice show signs of decline necessitating humane euthanasia, an overall survival (OS) event was recorded.

Ex vivo colony formation of circulating tumor cells (CTCs).

Whole blood was collected in heparinized tubes via cardiac puncture of tumor bearing $PyMT^+$ mice. All *in vivo* treatments began at 8 weeks of age and ended at 10 weeks of age. At 10 weeks, mice were euthanized, and blood was collected. 500 μL of whole blood was plated in a 15 cm tissue culture treated plate with 25 mL of DMEM high glucose (Corning; Cat#10–017-CV). For three days, the culture medium was agitated using figure eight movements to facilitate resuspension of non-attached cells, centrifuged at 1200 rpm for 5 minutes, supernatant was removed, and the cell pellet was added back to the original plate with fresh 25 mL of culture medium. By day 4, the fraction of non-attached cells was minimal, and the medium was aspirated and replaced with fresh medium. Following 10 more days in culture, plates were fixed with 100% methanol, stained with 0.5% crystal violet, and colonies with epithelial morphology were counted and compared between treatment groups. As a control, blood from non-tumor bearing mice was cultured and processed in parallel.

Cholesterol Assay.

To determine intracellular levels of cholesterol, we utilized the Amplex Red Cholesterol Assay Kit (Invitrogen; Cat#A12216) on cell extracts normalized by protein concentration.

Tail vein injection of tumor cells.

2 million R7 BC cells suspended in sterile PBS were injected into the tail vein of FVB/n wild-type mice. Mice received Atorvastatin treatment (20 mg/kg/day by oral gavage) starting 3 days prior and for 16 days after cell injection. After 16days, mice were euthanized and lung tissue harvested. Lungs were formalin fixed, paraffin-embedded, sectioned, and relative area of pathologic versus healthy tissue was quantified using ImageJ measurement tools. Groups were compared using Fisher's exact test.

Glycolysis Stress Test.

Glycolysis stress testing was performed using a Seahorse XFe96 Analyzer (Agilent) as previously described (36). For each experiment, 4,000 cells were plated in Seahorse XFe96 plates (Agilent) and allowed to attach overnight. For inhibitor treatment experiments, media was replaced with media containing inhibitor for 6 hours. Media was aspirated, wells washed with PBS, and then 100 μL of sterile 1X Krebs-Henseleit Buffer (KHB) was added to each well for 2 hours prior to the assay period. 10 mM glucose, 1 μM oligomycin, and 10 mM 2-deoxyglucose (2-DG) were added sequentially via the assay ports with automatic mixing and three readings taken per assay stage.

RNA and Protein Gene Expression Analyses.

RNA was extracted using a TRIzol (Invitrogen; Cat#15596018) as previously described (37). The High-Capacity cDNA Reverse Transcription Kit (Applied Biosystems; Cat#4368814) was used for cDNA synthesis. Target genes were normalized to ribosomal 18S expression using the $\Delta\Delta C_t$ method. Primer lists are provided in Supplemental Table S1. For protein expression analysis by western blot analysis, cell lysates were obtained using standard RIPA buffer containing cOmplete Protease Inhibitor Cocktail (Roche Cat#11 836 153 001) and PhosSTOP Phosphatase Inhibitor Cocktail (Roche #04 906 837 001). Antibodies used are listed in Supplemental Table S2.

Transcriptomics-based pathway enrichment analysis.

The T47D isogenic RON-modulated dataset (GEO Accession #GSE166575) has been previously described (21). The Enrichr software suite (38–40) was used to generate lists of enriched transcription factors and pathways based on differentially expressed genes using a False Discovery Rate (FDR) control of $q < 0.05$. Hits were plotted and ranked based off enrichment score. Hits were validated experimentally.

Mammosphere Formation Assays.

50,000 cells were plated in 6-well plates coated with 2 mL of 1% agarose for non-adherent culture (Day 0) as previously described (28). At Days 3 and 7, additional media was added with the respective treatments described. Images from individual wells were captured using an Axiovert S100TV microscope (Zeiss) on Day 10. Scale bar calibration and diameter measurements using the line function of ImageJ were employed for determining the number of mammospheres ≥50 microns. Experiments were normalized to the vehicle/untreated, RON-overexpressing samples.

Stable Isotope Resolved Metabolomics (SIRM).

Media preparation: powder DMEM lacking phenol red, glucose, glutamine, and sodium bicarbonate was prepared as described by the manufacturer (Corning; Cat#90-113-PB) with the addition of 3.0 g/L sodium bicarbonate, 5 μM ^{13}C-Glucose (Cambridge Isotope Laboratories; Cat#110187-42-3), 2 μM glutamine (Corning; Cat#25-005-CI), 5% (v/v) dialyzed fetal bovine serum (Gibco; Cat#A33820-01), and 1% (v/v) Gentamicin (Gibco; Cat#15710-064). Unlabeled controls (n=2 per group) received an equal concentration of ^{12}C-glucose (5 mM) with the same media composition.

Water soluble (polar phase) analysis: Ice cold MeOH:H_2O (80:20) was used to facilitate cell scraping and collection. Protein was pelleted out by centrifugation at 5725 × *g* for 5 minutes at 4°C. Following removal of the aqueous phase (polar metabolites), the protein pellet was washed with 0.5 mL of 100% MeOH, vortexed, and subjected to centrifugation at 2000 × *g* for 5 minutes at 4°C. The remaining MeOH supernatant was discarded. The polar metabolites and protein pellet solvents were evaporated in a SpeedVac device. Protein was quantified using BCA (BioRad; Cat#s 500–0113, 500–0114, 500–0115) and used for normalization after resuspension in 30 μL of RIPA buffer.

Lipid (non-polar phase) analysis: After 24 h of incubation, cells were quenched with ice cold acetonitrile, and nanopure water was added (acetonitrile/water at 2:1.5 by volume) to facilitate cell scraping and collection. Polar and non-polar metabolites were extracted via the solvent partition method using acetonitrile: water: chloroform at ratios 2: 1.5: 1 by volume (19). The aqueous phase (polar metabolites) and the organic phase (non-polar metabolites) were either lyophilized (CentriVap Labconco) or evaporated in a SpeedVac device, respectively. The protein residue was quantified using BCA and used for normalization. The NMR spectroscopy protocol has been previously described (41). Cholesterol peaks corresponding with C18H3 and C19H3 positions were internally normalized with the methanol resonance at 3.30 ppm and the ^{13}C-cholesterol groups were analyzed and compared across cell lines.

Statistical Analysis

Statistical significance was determined by performing Student's t-test for pairwise comparisons or ANOVA for comparison of multiple groups; data are expressed as mean ± standard deviation (SD). Significance (*) was set at $P<0.05$. Metastasis incidence was analyzed using Fisher's Exact test. Statistical tests were selected based on population distribution, data scale, and sample centrality/variability to meet assumptions of tests and thus represent appropriate assumptions. Variance between sample groups were found to be similar as tested by ANOVA.

RESULTS

Oncogenic RON signaling supports breast cancer recurrence and progression.

Recently, we showed that mammary tumors from PyMT mice show progressive increases in RON expression (42). Further, we showed that BMS777607, a receptor tyrosine kinase inhibitor that targets RON, treatment of PyMT mice leads to a plateau in primary tumor

growth and ablated metastatic incidence (42). Metastatic progression is a function of primary tumor growth, thus the question of whether the lack of metastasis was a direct or indirect result of BMS777607 treatment on primary tumor growth remained unanswered. To test the effects of RON signaling on metastatic progression, PyMT mice were treated daily with vehicle or BMS777607 starting at 8 weeks for two weeks (Figure 1A). During this timeframe, vehicle and PyMT mice exhibited a similar primary tumor burden (Supplemental Figure S1A). At 10 weeks, blood samples were collected and colony formation assays for circulating tumor cells (CTCs) were performed. As observed in Figure 1B and 1C, a significant reduction in breast cancer colony formation was observed in samples from mice where RON was chemically inhibited with BMS777607 (Figure 1B, 1C). Thus, under conditions wherein primary tumor growth is comparable, RON inhibition by BMS777607 treatment showed a reduction in cancer cell extravasation.

To further examine the role of RON in recurrence, we utilized an orthotopic transplantation model. In this model, RON-expressing mammary tumor cells (RL3T1 cells) were implanted into the #4 mammary gland of syngeneic immunocompetent female FVB mice. Once tumors reached 1000 mm^3, the entire tumor bearing mammary gland was surgically resected. Following primary tumor resection, no residual disease was detected by imaging (Figure 1D, 1E) and mice were subsequently imaged weekly for signs of breast cancer recurrence. At the first sign of recurrent signal detection, a relapse-free survival (RFS) event was recorded. When mice show signs of decline necessitating humane euthanasia, an overall survival (OS) event was recorded. Recurrent tumors from this model had a bias towards recurrence in the omentum and intestinal track (Supplemental Figure S1B). To experimentally test the role of RON signaling in breast cancer recurrence, RON inhibition was provided in an adjuvant setting through BMS777607 treatment (versus vehicle control) or through doxycycline (DOX) inducible shRNA to RON (versus mice not receiving DOX; see Supplemental Figure S1C). Strikingly, none of the BMS777607 treated mice (Figure 1D) or mice receiving DOX (Figure 1E) exhibited breast cancer recurrence while about half of the corresponding control mice (Vehicle, 71%, Figure 1D; No DOX, 40%, Figure 1E) relapsed within six weeks of resection. This was mirrored by OS (Figure 1D, E). Taken together, these data support that RON directly promotes recurrence.

RON expressing breast cancer cells upregulate glycolysis and cholesterol biosynthesis (CBS).

Previously, we reported pathway/gene ontology analyses of RON expressing human T47D breast cancer cells relative to T47D cells with a RON knockdown (21). This analysis identified enrichment of glycolysis, cholesterol biosynthesis (CBS) pathways, and SREBP signaling with RON expression. Herein, we confirmed prior RNASeq analysis examining the upregulation of CBS genes at the mRNA level (Supplemental Figure S2A). Protein level expression of glycolysis and CBS genes was also found to be upregulated in several RON expressing breast cancer cell lines including human MCF7 (control, PCI-EV and RON expressing, PCI-RON) and T47D (control shNT, RON knockdown, shRON) and murine R7 cells (control and with a CRISPR knockdown, sgRON) (Figure 2A).

To confirm upregulated glycolytic activity, we used the Seahorse metabolic flux analysis under glycolysis stress conditions. Consistently enhanced glycolytic flux in RON expressing R7 Control or MCF7 PCI-RON cells (Figure 2B) was observed compared to the corresponding isogenic RON deplete counterparts. Moreover, R7 Control cells showed impaired glycolytic flux with BMS777607 treatment, and BMS777607 treatment caused R7 Control cells to resemble untreated R7 sgRON cells. As expected, cells treated with the lactate dehydrogenase inhibitor, FX-11, showed reduced glycolytic flux (Figure 2C). Corresponding effects on the oxygen consumption rate wherein R7 Control and MCF7 PCI-RON cells have elevated oxygen consumption are shown in Supplemental Figure S2B, S2C. To rule out the possibility that these treatment conditions caused cytotoxicity that is in turn responsible for metabolic changes, we set up parallel cell cultures with identical treatment conditions and quantified live cell numbers with Trypan blue cell exclusion (Supplemental Figure S2D). To further complement the Seahorse data, we quantified incorporation of uniformly labeled ^{13}C-glucose carbons into glycolytic byproducts (3C-lactate, alanine) (Figure 2D). R7 Control cells show significantly upregulated incorporation of labeled carbons into each of the glycolytic byproduct pools and into cholesterol (Figure 2E), supporting the Seahorse results and suggesting that the upregulated glycolytic flux supports CBS. A model of these pathway interactions is shown in Figure 2F. Importantly, R7 Control and R7 sgRON cells showed no difference in cell growth kinetics under the conditions used for the Seahorse and metabolomics experiments (Supplemental Figure S2E).

RON-mediated upregulation of glycolysis and CBS is critical for RON augmented breast cancer stem cell self-renewal and breast cancer recurrence/progression.

Cancer stem cells (CSCs) play a role in metastasis/recurrence (43). To examine effects of glycolysis and CBS function on RON-driven cancer stem cell self-renewal, mammosphere formation assays (44) were performed in the presence and absence of the lactate dehydrogenase inhibitor, FX-11, and the HMG-CoA reductase inhibitor, atorvastatin. Images of mammospheres can be seen in Supplemental Figure S3A. Treatment with FX-11 or atorvastatin caused a reduction of mammosphere formation in R7 Control cells and MCF7 PCI-RON cells. Further, this reduction resembled mammosphere formation of their low RON expressing isogenic counterparts, which show no change to mammosphere formation under inhibitor treatment (Figure 3A, 3B; Supplemental Figure S3B, S3C). Our data support that glycolytic metabolites are used for cholesterol production to a greater extent in RON overexpressing cells suggesting a functional link between the upregulation of these pathways such that glycolysis inhibition consequences may be rescued by cholesterol supplementation. Indeed, supplementation of cholesterol restored mammosphere formation to that of vehicle treated levels (Figure 3A, 3B). Taken together, these data support that cholesterol is a critical effector molecule for RON-augmented mammosphere formation.

Given the safe and broad use of statins to target CBS in patients with hyperlipidemia, and our data supporting a link between glycolytic flux and CBS in RON expressing breast cancer cells, we reasoned that targeting RON-augmented CBS via well-optimized and well-tolerated statins has high potential for clinical translation. Thus, we tested the use of atorvastatin to inhibit RON-augmented CBS and metastasis in our murine models. Treatment of PyMT mice, which have progressive RON expression (25, 33), with atorvastatin showed

no effect on primary mammary tumor growth kinetics (Figure 3C). Strikingly, however, atorvastatin treated mice showed a significant reduction in lung metastasis compared to vehicle treated mice (Figure 3D). Correspondingly, atorvastatin treated mice showed a significant reduction in *ex vivo* CTC colony formation (Figure 3E, 3F). We next applied atorvastatin treatment to the murine recurrence model to examine consequences on recurrence in RON expressing breast cancers *in vivo*. Similar to the RON targeted approaches in Figure 1, nearly half of all vehicle treated mice (43%), but none of the atorvastatin treated mice (0%) showed breast cancer recurrence (Figure 3G). Taken together, these data show that CBS pathways are critical for RON-augmented metastatic progression recurrence in syngeneic murine models of breast cancer.

c-Myc and SREBP2 transcription factors regulate RON-dependent glycolysis and CBS gene expression, respectively.

To identify RON dependent mechanisms involved in glycolysis and CBS, we employed the Enrichr bioinformatics tool wherein differentially expressed genes based on RON absence or presence (using a 5-fold cutoff to define differential expression) were submitted. Output from Enrichr provides list of probable active transcription factors with enrichment scores that are calculated from the adjusted P-value and Odds Ratio. We performed Enrichr analysis on RNAseq data from RON-modulated T47D cells (shNT versus shRON) cells (21); prior analysis using ToppGene had already implicated SREBP signaling. Given the prior hit of SREBP signaling in published analyses (21), its known role as a master regulator of cholesterol biosynthesis genes, and its hit via Enrichr, we reasoned it was likely to participate in the mechanism for upregulated CBS. Similarly reasoned, c-Myc was previously shown to be upregulated in RON-driven breast cancer (24) and appears as significant hits in using Enrichr, and is a known master regulator of numerous metabolic processes (Figure 4A).

To confirm RON-dependent SREBP2 expression, we quantified SREBP2 gene expression in R7 Control and R7 sgRON cells with and without RON inhibition by BMS777607 treatment. R7 sgRON cells harbored reduced basal levels of SREBP2 expression compared with R7 Control cells, and BMS777607 treatment reduced SREBP2 expression levels in R7 Control cells to those of R7 sgRON cells. R7 sgRON cells with BMS777607 treatment showed comparable SREBP2 expression to its untreated counterpart thus indicating RON selectivity of the inhibitor (Figure 4B). Overexpression of SREBP2 in R7 sgRON cells resulted in enhanced expression of the CBS genes LSS and FDFT1 but did not alter c-Myc and HK2 levels (Figure 4C) and showed enhanced levels of intracellular cholesterol (Supplemental Figure S4). Importantly, SREBP2 overexpression also enhanced mammosphere formation by roughly 2-fold (Figure 4D). Taken together, these data further support the role of cholesterol production in supporting breast cancer stem cell self-renewal and implicate SREBP2 as a critical regulatory transcription factor downstream from RON.

To confirm the upregulation of c-Myc by RON, we quantified c-Myc expression in RON-modulated MCF7, T47D, and R7 cells. We found c-Myc consistently upregulated in RON expressing samples relative to their isogenic counterparts that expressed low levels of RON (Figure 4E). To examine the function of c-Myc as a regulator of glycolysis

gene expression downstream of RON, we knocked down c-Myc in R7 Control cells or overexpressed c-Myc in R7 sgRON cells and measured the expression of the glycolysis enzymes HK2 and LDHA. When c-Myc was knocked down in RON expressing cells, HK2 and LDHA levels were reduced; when c-Myc was overexpressed in cells with low RON expression, HK2 and LDHA levels were induced (Figure 4F). Of note, SREBP2 and LSS expression patterns in the c-Myc-modulated cells remain relatively unchanged, suggesting that c-Myc and SREBP2 are unlikely to be interacting. Knockdown of c-Myc in RON overexpressing cells showed a roughly 2-fold reduction in mammosphere formation (Figure 4G) similar to cells wherein RON is targeted (see Supplemental Figure S3B, 3D). Interestingly, c-Myc overexpression in R7 sgRON cells did not stimulate mammosphere formation relative to control (Figure 4H), indicating that c-Myc is not sufficient to drive mammosphere formation under conditions with RON loss. These data support a model wherein RON overexpression leads to c-Myc-dependent glycolysis gene expression which supports mammosphere formation in conjunction with elevated CBS gene expression.

RON-dependent β-catenin signaling regulates SREBP2-driven CBS gene expression.

To define signaling pathways downstream from RON and upstream from c-Myc and SREBP2, we again utilized the Enrichr-based analysis of RON-modulated T47D cells and noted pathway enrichment via KEGG and WikiPathways signatures. This analysis used a list of differentially expressed genes based on the presence or absence of RON, but the output is probable active pathways ranked by Enrichment scores. Across the two analyses, two pathway hits that are known to be activated by RON were found: MAPK and β-catenin pathways (Figure 5A).

To confirm β-catenin activation, we examined expression of the known β-catenin target genes, *Ccnb1* and *Ect2*, in R7 Control and R7 sgRON cells. Indeed, reduced expression was evident (Figure 5B). To further examine transcription factor responses downstream from β-catenin activation, we utilized a cell line derived from a mammary tumor of MMTV-RON (MR) mouse containing a β-catenin floxed allele (29), referred to as MRBC cells. MRBC cells treated with a Cre-recombinase expressing adenovirus (Ad-Cre) were stably derived from parental MRBC cells generating β-catenin$^{-/-}$ cells (referred to as MRBC−/− cells, Figure 5C). Previously, our laboratory showed that RON promotes the non-canonical activation β-catenin by phosphorylating tyrosines 654 (Y654) and 670 (Y670) of β-catenin. Further, we showed that β-catenin Y654 and Y670 were crucial for breast cancer stem cell properties downstream of RON (28, 29). To discern the importance of RON induced β-catenin Y654/Y670 phosphorylation on SREBP2, we stably expressed β-catenin^{WT} or β-catenin$^{Y654F/Y670F}$ (Double Mutant; DM) in MRBC β-catenin$^{-/-}$ cells (Figure 5C). Protein expression of these RON-overexpressing, β-catenin modulated cells showed that loss of β-catenin reduced levels of cleaved SREBP2, which were largely restored under WT β-catenin rescue, but not DM β-catenin rescue despite a larger transfection efficiency of the DM construct (Figure 5C). Similarly, CBS genes, LSS and FDFT1, showed reduced expression when β-catenin expression was lost, and were rescued by the WT but not DM construct. c-Myc expression levels were relatively unchanged suggesting that c-Myc is not regulated by β-catenin which is consistent with LDHA expression patterns. ERK1/2 activation patterns based on β-catenin status similarly showed a lack of regulation.

To complement these studies, we utilized LiCl treatment to activate β-catenin (30, 45). R7 sgRON cells with β-catenin activation via LiCl showed induction of SREBP2 (Supplemental Figure S5A). Moreover, R7 sgRON cells with β-catenin activation via LiCl also showed enhanced expression of CBS genes (Supplemental Figure S5B). Taken together, our data support a model wherein RON overexpression activates β-catenin through Y654/Y670 phosphorylation to stimulate SREBP2 expression. Given that our previous studies have demonstrated the role of β-catenin activation through Y654/Y670 by RON to support mammosphere formation (28), we focused on the functional role of β-catenin dependent SREBP2 expression on mammosphere formation. MRBC β-catenin$^{-/-}$ cells (MRBC$^{-/-}$ cells) with or without SREBP2 overexpression were generated. REBP2 overexpression in these cells enhanced levels of the CBS genes LSS and FDFT1, with no change to c-Myc or HK2 expression (Figure 5D). Mammosphere formation was also significantly induced in MRBC$^{-/-}$ cells harboring overexpressed SREBP2 supporting the functional importance of SREBP2 downstream from β-catenin (Figure 5E).

RON-dependent MAPK signaling stimulates c-Myc-driven glycolysis gene expression

To confirm MAPK upregulation by RON, we evaluated ERK1/2 activation in RON-overexpressing MCF7 cells (PCI-RON) compared with empty vector controls (PCI-EV). These cells show significant P-ERK1/2 accumulation over their isogenic counterparts (Figure 5F). To examine the consequences of MAPK activation, we expressed a Constitutively Active form of MEK1 (CA-MEK1), an upstream activator of ERK1/2, in R7 sgRON cells. We confirmed activation of phosphorylated ERK1/2 (P-ERK 1/2), which coincided with elevated c-Myc, HK2, and LDHA expression without significant changes in cleaved SREBP2, LSS, or β-catenin, suggesting that ERK and c-Myc signaling pathways work independently (Figure 5G). Similar results were obtained using R7 cells with ERK1/2 inhibition using Ravoxertinib; c-Myc, HK2, and LDHA expression were diminished without impacting LSS or SREBP2 expression (Figure 5H). Finally, mammosphere formation of R7 cells in the presence of Ravoxertinib showed a significant reduction, functionally supporting ERK1/2 MAPK as a key pathway in this RON-driven model (Figure 5I).

Our data provide evidence of two pathway arms wherein RON drives mammosphere formation dependent on augmented glycolysis and CBS. RON-dependent activation of ERK1/2 enhances glycolysis through c-Myc dependent upregulation of glycolysis genes. In parallel, RON-dependent non-canonical β-catenin activation enhances CBS through SREBP2-dependent upregulation of CBS genes. Thus, RON activation of glycolysis and CBS pathway arms allows for robust cholesterol production through glycolysis-dependent substrate production utilized by upregulated CBS genes. Our model is summarized in Figure 6.

DISCUSSION

The data presented here builds on the relationship between RON expression and patient survival, metastatic progression, and recurrence in in breast cancer patients (8, 9). Given the lack of association between RON expression and breast cancer subtype (9), and that recurrence occurs in all breast cancer subtypes (10), RON may be a significant target

for improving breast cancer outcomes. Our data provide direct pre-clinical evidence that targeting RON improves breast cancer outcomes driven by recurrence and metastasis: genetic or pharmacologic targeting of RON abrogates formation of recurrent tumors from the treated primary tumors. Moreover, *in vivo* treatment with the RON inhibitor BMS777607 reduced the *ex vivo* colony formation of whole blood-derived circulating tumor cells (CTCs), further supporting the reduction in recurrence potential. Thus, BMS777607 is a potential RON-targeting therapy that may prevent metastasis and recurrence, which are responsible for the vast majority of breast cancer related mortality. Completion of a Phase I trial of BMS777607 efficacy in advanced/metastatic solid tumors further elevates feasibility for further clinical trials (18). Moreover, these data supported reduced expression of bone turnover in postmenopausal women; bone destruction through metastasis in breast cancer is a symptom of progressive disease. However, there are currently no clinical trials of BMS777607 or other RON inhibitors listed specifically for breast cancer, and a possible survival benefit resulting from the targeting of RON has therefore not yet been tested.

Transcriptomic data indicated enrichment of metabolic processes including glycolysis and cholesterol biosynthesis (CBS). Given the existing literature that links metabolic reprogramming to breast cancer metastasis (19, 20), we posited that glycolysis and CBS are plausible biological processes to support metastatic progression and recurrence. We confirmed the upregulation of glycolytic flux and cholesterol and found that outputs of glycolysis include substrate that can be used in cholesterol production.

BCSCs are a subpopulation within the tumor that harbors tumor initiation/repopulation capabilities that are considered drivers of recurrence (43). At the doses used here, RON-overexpressing breast cancer cells showed sensitivity to inhibition of glycolysis or CBS whereas their low RON expressing isogenic counterparts were unaffected. Moreover, the reversibility of either glycolysis inhibition or CBS inhibition by cholesterol supplementation suggests that cholesterol production is the critical outcome of both pathways and provides a functional link to pathway interactions supported by SIRM data. Mechanistic interrogation of components downstream from RON that regulate glycolysis and CBS gene expression revealed two parallel pathways that each regulate a separate arm: MAPK-dependent c-Myc expression and β-catenin$^{Y654/Y670}$-dependent SREBP2 expression, respectively. c-Myc overexpression in RON-deplete cells was not sufficient for inducing mammosphere formation whereas SREBP2 overexpression significantly induced mammopshere formation in RON deplete cells. These results are consistent with the rescue of mammosphere formation by cholesterol supplementation under glycolysis inhibition conditions. These results suggest that while glycolysis supports cholesterol production, hyperactivation of CBS alone is sufficient for enhanced mammosphere formation.

Given broad use of statins for the treatment of hyperlipidemia, we chose to follow the CBS inhibition route for *in vivo* testing. Strikingly, atorvastatin treatment had no effect on primary tumor growth kinetics in the PyMT model but impaired metastatic progression. Moreover, atorvastatin abrogated recurrence when given in an adjuvant setting in our recurrence model. Together, these data suggest that cholesterol synthesis via glycolysis-driven substrate production and elevated CBS enzyme expression is critical for the ability of RON to drive metastatic progression and recurrence.

In addition to cholesterol biosynthetic pathways, statins inhibit the mevalonate pathway due to the shared use of HMG-CoA Reductase to produce necessary substrate. The mevalonate pathway has been shown to support BCSCs, particularly in basal-like breast cancer (46), and promotes resistance to anti-HER2 therapy (47). These pleiotropic effects of statins (48) suggest that cancers that utilize cholesterol or the mevalonate pathway more generally may show benefit for breast cancer patients, but are most useful when biomarkers to predict response and guide use are known. Within our studies herein, gene expression supports cholesterol pathways and mevalonate pathways are potentially being upregulated by RON, however, the use of cholesterol to rescue mammosphere formation suggests cholesterol is a critical molecular output. Further experimentation would be useful to define independent roles of CBS and mevalonate pathways.

With respect to clinical testing, statin treatment for breast cancer appears to be gaining traction, as numerous breast cancer clinical trials with single or combination treatment with statins are currently recruiting. Preclinical models support that statin use, especially lipophilic statins such as atorvastatin, reduce breast cancer metastasis and recurrence outcomes (12, 13), as is supported by data herein. The data presented herein serve to fortify these efforts, and further suggest that RON expression may be a biomarker for response to statins in breast cancer. We hope these data provide urgency to examine the expression of RON as a clinical biomarker of statin response.

Supplementary Material

Refer to Web version on PubMed Central for supplementary material.

ACKNOWLEDGMENTS

We would like to thank Lisa Privette-Vinnedge and Megan Johnstone for their guidance and technical assistance. This research was funded by NCI T32 CA117846 (SEW and JCD), F31 CA228373 (BGH and SEW), NCI R01 CA239697 (SEW and SIW), and US Department of Veterans Affairs grant 1IOBX000803 (SEW).

DATA AVAILABILITY

The datasets analyzed during the current study are available in the Gene Expression Omnibus repository (GSE162532) and available upon request.

REFERENCES

1. ACS. Breast Cancer Facts & Figures 2017–2018. 2017.
2. ACS. Cancer Facts & Figures. 2019.
3. Narod SA, Iqbal J, Miller AB. Why have breast cancer mortality rates declined? Journal of Cancer Policy. 2015;5:8–17.
4. CRUK. Cancer Statistics for the UK.
5. Colzani E, Johansson ALV, Liljegren A, Foukakis T, Clements M, Adolfsson J, et al. Time-dependent risk of developing distant metastasis in breast cancer patients according to treatment, age and tumour characteristics. British Journal of Cancer. 2014;110(5):1378–84. [PubMed: 24434426]
6. Esserman LJ, Thompson IM, Reid B. Overdiagnosis and overtreatment in cancer: an opportunity for improvement. Jama. 2013;310(8):797–8. [PubMed: 23896967]

7. Maggiora P, Marchio S, Stella MC, Giai M, Belfiore A, De Bortoli M, et al. Overexpression of the RON gene in human breast carcinoma. Oncogene. 1998;16:2927–33. [PubMed: 9671413]
8. Lee W-Y, Chen HHW, Chow N-H, Su W-C, Lin P-W, Guo H-R. Prognostic significance of co-expression of RON and MET receptors in node-negative breast cancer patients. Clinical Cancer Research. 2005;11(6):2222–8. [PubMed: 15788670]
9. Hunt BG, Wicker CA, Bourn JR, Lower EE, Takiar V, Waltz SE. MST1R (RON) expression is a novel prognostic biomarker for metastatic progression in breast cancer patients. Breast Cancer Research and Treatment. 2020.
10. van Maaren MC, de Munck L, Strobbe LJA, Sonke GS, Westenend PJ, Smidt ML, et al. Ten-year recurrence rates for breast cancer subtypes in the Netherlands: A large population-based study. International journal of cancer. 2019;144(2):263–72. [PubMed: 30368776]
11. Ahern TP, Lash TL, Damkier P, Christiansen PM, Cronin-Fenton DP. Statins and breast cancer prognosis: evidence and opportunities. The Lancet Oncology. 2014;15(10):e461–e8. [PubMed: 25186049]
12. Campbell MJ, Esserman LJ, Zhou Y, Shoemaker M, Lobo M, Borman E, et al. Breast Cancer Growth Prevention by Statins. Cancer Research. 2006;66(17):8707–14. [PubMed: 16951186]
13. Beckwitt CH, Clark AM, Ma B, Whaley D, Oltvai ZN, Wells A. Statins attenuate outgrowth of breast cancer metastases. British Journal of Cancer. 2018;119(9):1094–105. [PubMed: 30401978]
14. Van Wyhe RD, Rahal OM, Woodward WA. Effect of statins on breast cancer recurrence and mortality: a review. Breast Cancer: Targets and Therapy. 2017;9:559.
15. Beckwitt CH, Brufsky A, Oltvai ZN, Wells A. Statin drugs to reduce breast cancer recurrence and mortality. Breast Cancer Research. 2018;20(1):144. [PubMed: 30458856]
16. Brindisi M, Fiorillo M, Frattaruolo L, Sotgia F, Lisanti MP, Cappello AR. Cholesterol and mevalonate: two metabolites involved in breast cancer progression and drug resistance through the ERRα pathway. Cells. 2020;9(8):1819. [PubMed: 32751976]
17. Nelson ER, Chang C-y, McDonnell DP. Cholesterol and breast cancer pathophysiology. Trends in Endocrinology & Metabolism. 2014;25(12):649–55. [PubMed: 25458418]
18. Andrade K, Fornetti J, Zhao L, Miller SC, Randall RL, Anderson N, et al. RON kinase: A target for treatment of cancer-induced bone destruction and osteoporosis. Science translational medicine. 2017;9(374):eaai9338. [PubMed: 28123075]
19. Parida PK, Marquez-Palencia M, Nair V, Kaushik AK, Kim K, Sudderth J, et al. Metabolic diversity within breast cancer brain-tropic cells determines metastatic fitness. Cell Metabolism. 2022;34(1):90–105.e7. [PubMed: 34986341]
20. Havas KM, Milchevskaya V, Radic K, Alladin A, Kafkia E, Garcia M, et al. Metabolic shifts in residual breast cancer drive tumor recurrence. The Journal of clinical investigation. 2017;127(6).
21. Bourn JR, Ruiz-Torres SJ, Hunt BG, Benight NM, Waltz SE. Tumor cell intrinsic RON signaling suppresses innate immune responses in breast cancer through inhibition of IRAK4 signaling. Cancer Letters. 2021;503:75–90. [PubMed: 33508385]
22. Bourn JR, Ruiz-Torres SJ, Hunt BG, Benight NM, Waltz SE. Tumor cell intrinsic RON signaling suppresses innate immune responses in breast cancer through inhibition of IRAK4 signaling. Cancer Lett. 2021;503:75–90. [PubMed: 33508385]
23. Wicha MS, Liu S, Dontu G. Cancer stem cells: an old idea—a paradigm shift. Cancer research. 2006;66(4):1883–90. [PubMed: 16488983]
24. Zinser GM, Leonis MA, Toney K, Pathrose P, Thobe M, Kader SA, et al. Mammary-specific Ron receptor overexpression induces highly metastatic mammary tumors associated with β-catenin activation. Cancer research. 2006;66(24):11967–74. [PubMed: 17178895]
25. Hunt BG, Jones A, Lester C, Davis JC, Benight NM, Waltz SE. RON (MST1R) and HGFL (MST1) Co-Overexpression Supports Breast Tumorigenesis through Autocrine and Paracrine Cellular Crosstalk. Cancers. 2022;14(10):2493. [PubMed: 35626096]
26. McClaine RJ, Marshall AM, Wagh PK, Waltz SE. Ron receptor tyrosine kinase activation confers resistance to tamoxifen in breast cancer cell lines. Neoplasia. 2010;12(8):650–8. [PubMed: 20689759]

27. Marshall AM, McClaine RJ, Gurusamy D, Gray JK, Lewnard KE, Khan SA, et al. Estrogen receptor alpha deletion enhances the metastatic phenotype of Ron overexpressing mammary tumors in mice. Mol Cancer. 2012;11(1):2. [PubMed: 22226043]
28. Ruiz-Torres SJ, Benight NM, Karns RA, Lower EE, Guan JL, Waltz SE. HGFL-mediated RON signaling supports breast cancer stem cell phenotypes via activation of non-canonical beta-catenin signaling. Oncotarget. 2017;8(35):58918–33. [PubMed: 28938607]
29. Wagh PK, Zinser GM, Gray JK, Shrestha A, Waltz SE. Conditional deletion of β-catenin in mammary epithelial cells of Ron receptor, Mst1r, overexpressing mice alters mammary tumorigenesis. Endocrinology. 2012;153(6):2735–46. [PubMed: 22474186]
30. Brown NE, Paluch AM, Nashu MA, Komurov K, Waltz SE. Tumor Cell Autonomous RON Receptor Expression Promotes Prostate Cancer Growth Under Conditions of Androgen Deprivation. Neoplasia. 2018;20(9):917–29. [PubMed: 30121008]
31. Gurusamy D, Gray JK, Pathrose P, Kulkarni RM, Finkleman FD, Waltz SE. Myeloidspecific expression of Ron receptor kinase promotes prostate tumor growth. Cancer Res. 2013;73(6):1752–63. [PubMed: 23328584]
32. Stuart WD, Kulkarni RM, Gray JK, Vasiliauskas J, Leonis MA, Waltz SE. Ron receptor regulates Kupffer cell-dependent cytokine production and hepatocyte survival following endotoxin exposure in mice. Hepatology. 2011;53(5):1618–28. [PubMed: 21520175]
33. Peace BE, Toney-Earley K, Collins MH, Waltz SE. Ron receptor signaling augments mammary tumor formation and metastasis in a murine model of breast cancer. Cancer Res. 2005;65(4):1285–93. [PubMed: 15735014]
34. Jiang H, Zheng H. Efficacy and adverse reaction to different doses of atorvastatin in the treatment of type II diabetes mellitus. Bioscience Reports. 2019;39(7):BSR20182371.
35. Faustino-Rocha A, Oliveira PA, Pinho-Oliveira J, Teixeira-Guedes C, Soares-Maia R, da Costa RG, et al. Estimation of rat mammary tumor volume using caliper and ultrasonography measurements. Lab Anim (NY). 2013;42(6):217–24. [PubMed: 23689461]
36. Teslaa T, Teitell MA. Techniques to Monitor Glycolysis. Elsevier; 2014. p. 91–114.
37. Sullivan C, Brown NE, Vasiliauskas J, Pathrose P, Starnes SL, Waltz SE. Prostate Epithelial RON Signaling Promotes M2 Macrophage Activation to Drive Prostate Tumor Growth and Progression. Molecular Cancer Research. 2020;18(8):1244–54. [PubMed: 32439702]
38. Xie Z, Bailey A, Kuleshov MV, Clarke DJB, Evangelista JE, Jenkins SL, et al. Gene Set Knowledge Discovery with Enrichr. Current Protocols. 2021;1(3):e90. [PubMed: 33780170]
39. Kuleshov MV, Jones MR, Rouillard AD, Fernandez NF, Duan Q, Wang Z, et al. Enrichr: a comprehensive gene set enrichment analysis web server 2016 update. Nucleic Acids Research. 2016;44(W1):W90–W7. [PubMed: 27141961]
40. Chen EY, Tan CM, Kou Y, Duan Q, Wang Z, Meirelles GV, et al. Enrichr: interactive and collaborative HTML5 gene list enrichment analysis tool. BMC Bioinformatics. 2013;14(1):128. [PubMed: 23586463]
41. Vicente-Munoz S, Hunt BG, Lange TE, Wells SI, Waltz SE. NMR-based metabolomic analysis identifies RON-DEK-beta-catenin dependent metabolic pathways and a gene signature that stratifies breast cancer patient survival. PLoS One. 2022;17(9):e0274128. [PubMed: 36067206]
42. Hunt BG, Jones A, Lester C, Davis JC, Benight NM, Waltz SE. RON (MST1R) and HGFL (MST1) Co-Overexpression Supports Breast Tumorigenesis through Autocrine and Paracrine Cellular Crosstalk. Cancers (Basel). 2022;14(10):2493. [PubMed: 35626096]
43. Chang JC. Cancer stem cells: Role in tumor growth, recurrence, metastasis, and treatment resistance. Medicine. 2016;95(Suppl 1).
44. Al-Hajj M, Wicha MS, Benito-Hernandez A, Morrison SJ, Clarke MF. Prospective identification of tumorigenic breast cancer cells. Proceedings of the National Academy of Sciences. 2003;100(7):3983–8.
45. Zhang F, Phiel CJ, Spece L, Gurvich N, Klein PS. Inhibitory phosphorylation of glycogen synthase kinase-3 (GSK-3) in response to lithium Evidence for autoregulation of GSK-3. Journal of Biological Chemistry. 2003;278(35):33067–77. [PubMed: 12796505]

46. Ginestier C, Monville F, Wicinski J, Cabaud O, Cervera N, Josselin E, et al. Mevalonate Metabolism Regulates Basal Breast Cancer Stem Cells and Is a Potential Therapeutic Target. Stem Cells. 2012;30(7):1327–37. [PubMed: 22605458]

47. Sethunath V, Hu H, De Angelis C, Veeraraghavan J, Qin L, Wang N, et al. Targeting the Mevalonate Pathway to Overcome Acquired Anti-HER2 Treatment Resistance in Breast Cancer. Molecular Cancer Research. 2019;17(11):2318–30. [PubMed: 31420371]

48. Borgquist S, Bjarnadottir O, Kimbung S, Ahern T. Statins: a role in breast cancer therapy? Journal of internal medicine. 2018;284(4):346–57. [PubMed: 29923256]

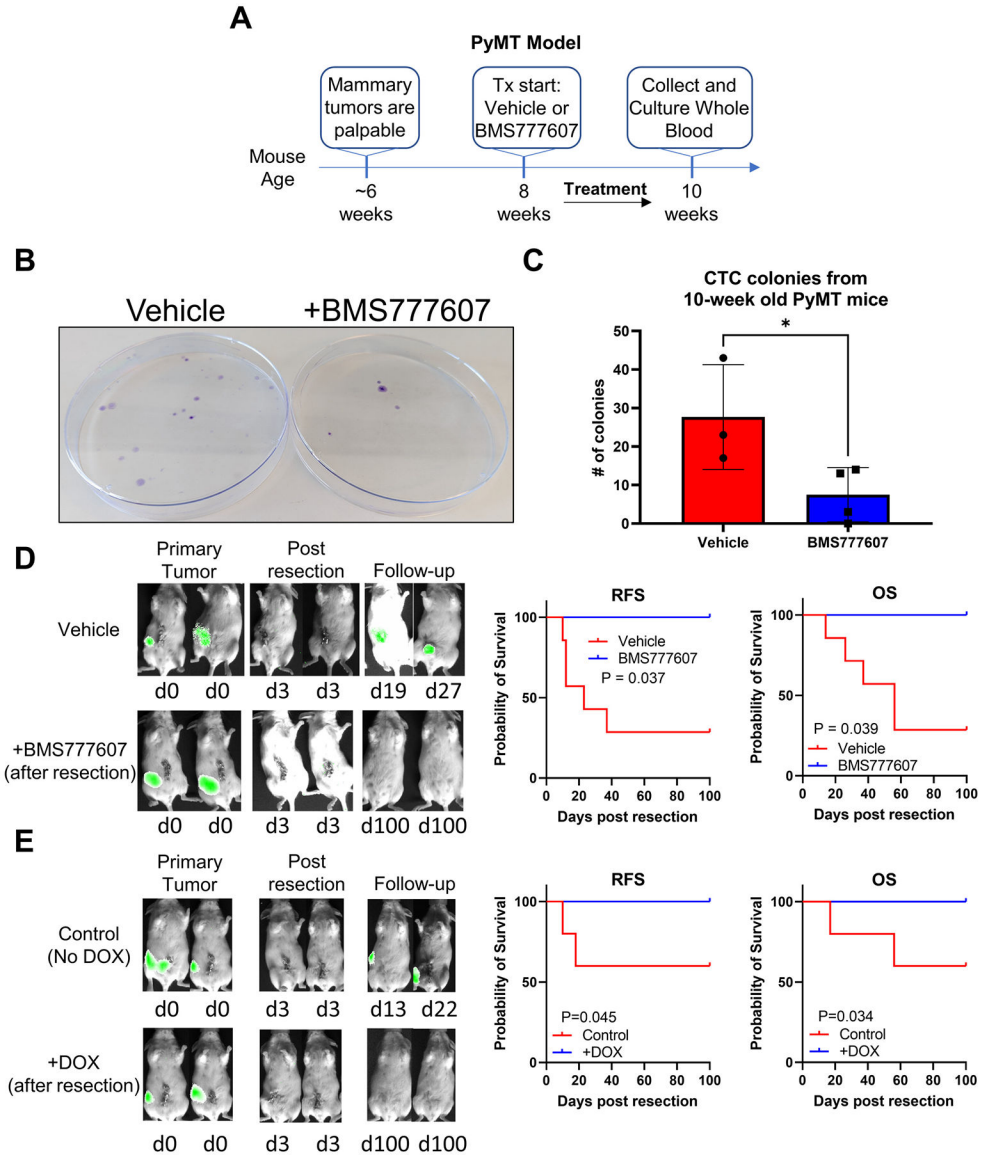

Figure 1. Inhibition or silencing of RON abrogates recurrence in murine breast cancer models.

(**A**) Workflow of PyMT mouse treatment and collection of whole blood for circulating tumor cell (CTC) *ex vivo* colony formation. (**B**) Representative image of CTCs colonies from *ex vivo* culture of whole blood from PyMT mice after two weeks of vehicle (n=3) or BMS777607 (n=4) treatment and (**C**) quantitation of CTC colonies (*P<0.05). Data displayed represent mean values ± SD. (**D**) Representative images of *in vivo* recurrence (left) of mice with orthotopically implanted, firefly luciferase-expressing RL3T1 cells that underwent tumor-bearing mammary gland resection and then began Vehicle (corn oil; n=7) or BMS777607 (50 mg/kg/day; n=4) treatment and monitored via *in vivo* imaging. Relapse-free survival (RFS; middle) and overall survival (OS; right) Kaplan-Meier curves with Log-Rank statistics. Follow-up images were taken on days: Vehicle, day 19 post resection and day 27 post resection; BMS777607, both 100 days post resection. (**E**) Representative images of *in vivo* recurrence (left) of mice with orthotopically implanted,

firefly luciferase-expressing, and doxycycline inducible shRON-expressing RL3T1 cells that underwent tumor-bearing mammary gland resection and then began Control (normal water; n=5) or +DOX (1 mg/mL ad libitum; n=9) treatment and monitored via *in vivo* imaging. RFS (middle) and OS (right) Kaplan-Meier curves with Log-Rank statistics. Follow-up images were taken on days: Control, day 13 post resection and day 20 post resection; +DOX, both 100 days post resection. Data displayed represent mean values ± SD. Ns, not significant; *P<0.05; **P<0.01; ***P<0.001; ****P<0.0001

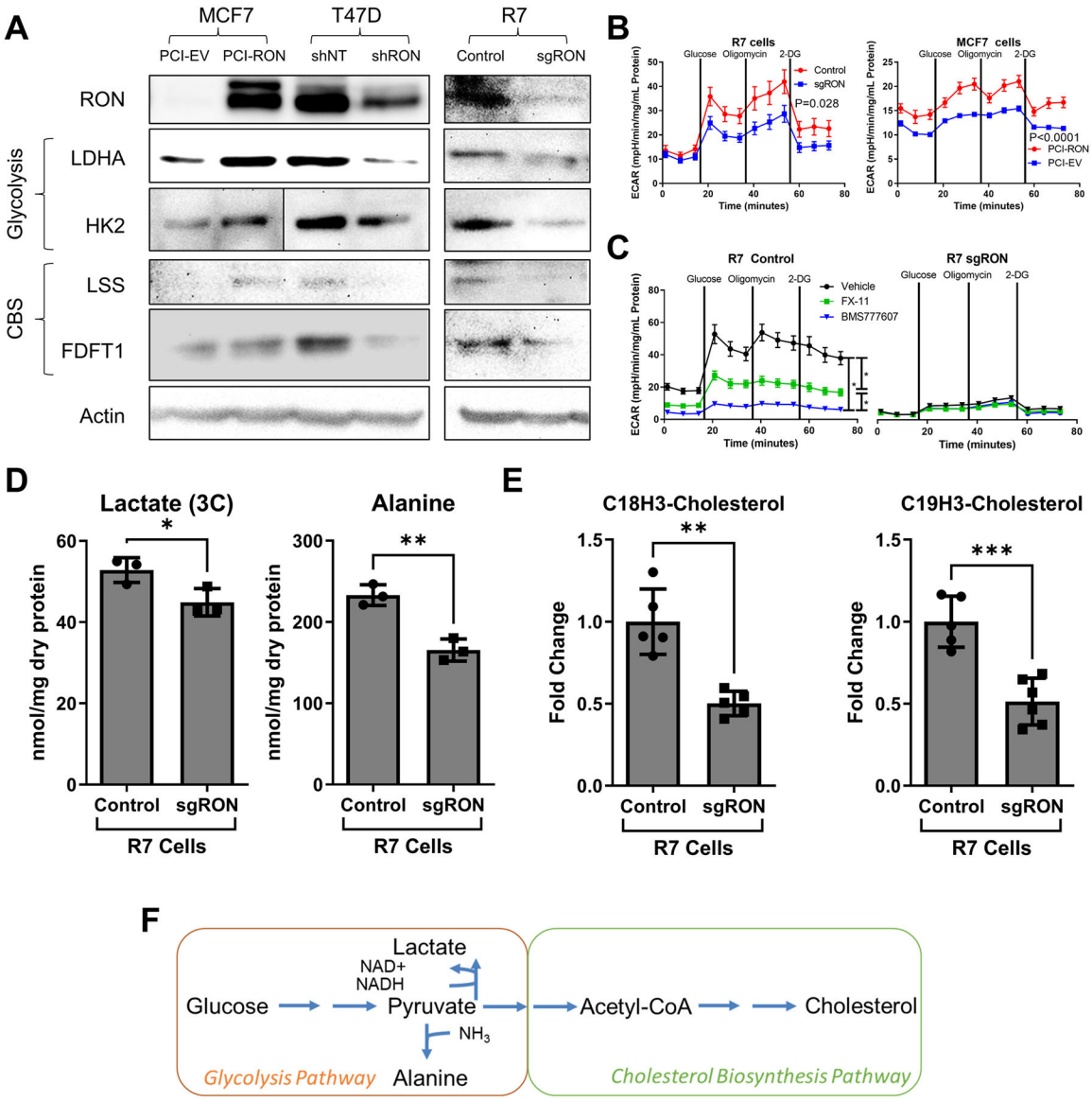

Figure 2. Cholesterol biosynthesis (CBS) and glycolytic flux are upregulated in RON-overexpressing breast cancer cells.

(**A**) Western blot analysis of CBS and glycolysis genes of RON-modulated isogenic breast cancer cell lines: MCF7, T47D, and R7. Black line between the MCF7 and T47D cells on HK2 blot denotes separate exposure times between MCF7 and T47D groups for HK2. Glycolysis stress test on the Seahorse metabolic flux platform of (**B**) RON-modulated R7 cells (n=3 biological replicates) and MCF7 cells (n=3 biological replicates) and (**C**) inhibitor-treated (RON inhibitor, BMS777607; LDH inhibitor, FX-11) R7 Control cells and R7 sgRON cells (n=3 biological replicates). (**D**) Stable isotope resolved metabolomic analysis of ^{13}C incorporation after 24-hour incubation with uniformly labeled ^{13}C-glucose examining incorporation into glycolytic endpoints lactate and alanine (n=3–4 each) and (**E**) incorporation of ^{13}C from glucose into intracellular cholesterol levels of RON-modulated R7 cells. (**F**) Glycolysis and CBS pathway interaction highlighting the function of glycolytic

flux in providing substrates for CBS. Western blot expression comparisons are only intended to be made within individual boxes. Data displayed represent mean values ± SD. *P<0.05; **P<0.01; ***P<0.001.

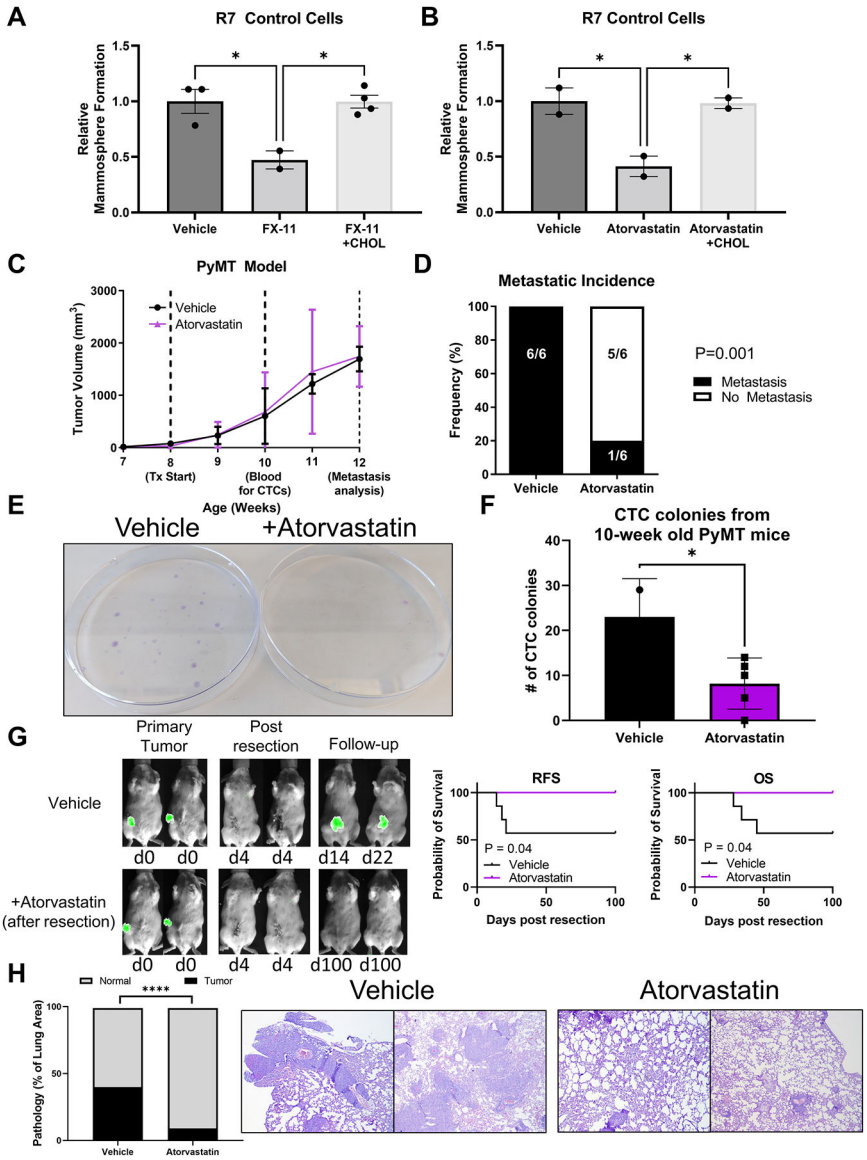

Figure 3. Statin-mediated CBS inhibition abrogates mammosphere formation and metastatic progression/recurrence in RON expressing breast cancer models.

Mammosphere formation of R7 Control cells under (**A**) 5 μM FX-11 (LDH inhibitor) treatment with or without 10 μM cholesterol rescue and (**B**) 500 nM atorvastatin (CBS inhibitor) with or without 10 μM cholesterol rescue; results are representative of one biological replicate (with similar effects observed in n=3 biological replicates). (**C**) Tumor growth kinetics of PyMT mice with 20 mg/kg/day atorvastatin (n=6) or vehicle (corn oil; n=6) treatment. (**D**) Metastatic incidence in lungs of mice that underwent vehicle (corn oil; n=6) or atorvastatin (n=6) treatment. (**E**) Representative image of CTCs colonies from *ex vivo* culture of whole blood from PyMT mice after two weeks of vehicle (n=3) or atorvastatin (n=5) treatment and (**F**) quantitation of CTC colonies. (**G**) Representative images of *in vivo* recurrence (left) of mice with orthotopically implanted, firefly luciferase-expressing RL3T1 cells that underwent tumor-bearing mammary gland resection and then began vehicle (corn oil; n=7) or atorvastatin (n=8) treatment and monitored via *in vivo*

imaging. Relapse-free survival (RFS; middle) and overall survival (OS; right) Kaplan-Meier curves with Log-Rank statistics. Follow-up images were taken on days: Vehicle, day 14 post resection and day 22 post resection; +DOX, both 100 days post resection. Tail vein injection of R7 cells and treatment of mice with or without Atorvastatin. Tissue was harvested 16 days post tumor cell injection. Lungs were sectioned and tumor bearing versus normal lung area was calculated from (n=4–6 lungs group). Two representative H&E images of lungs from both groups are displayed. Groups compared using Fisher's exact test. Data displayed represent mean values ± SD (except for A and B which show SEM). *P<0.05;****P<0.0001

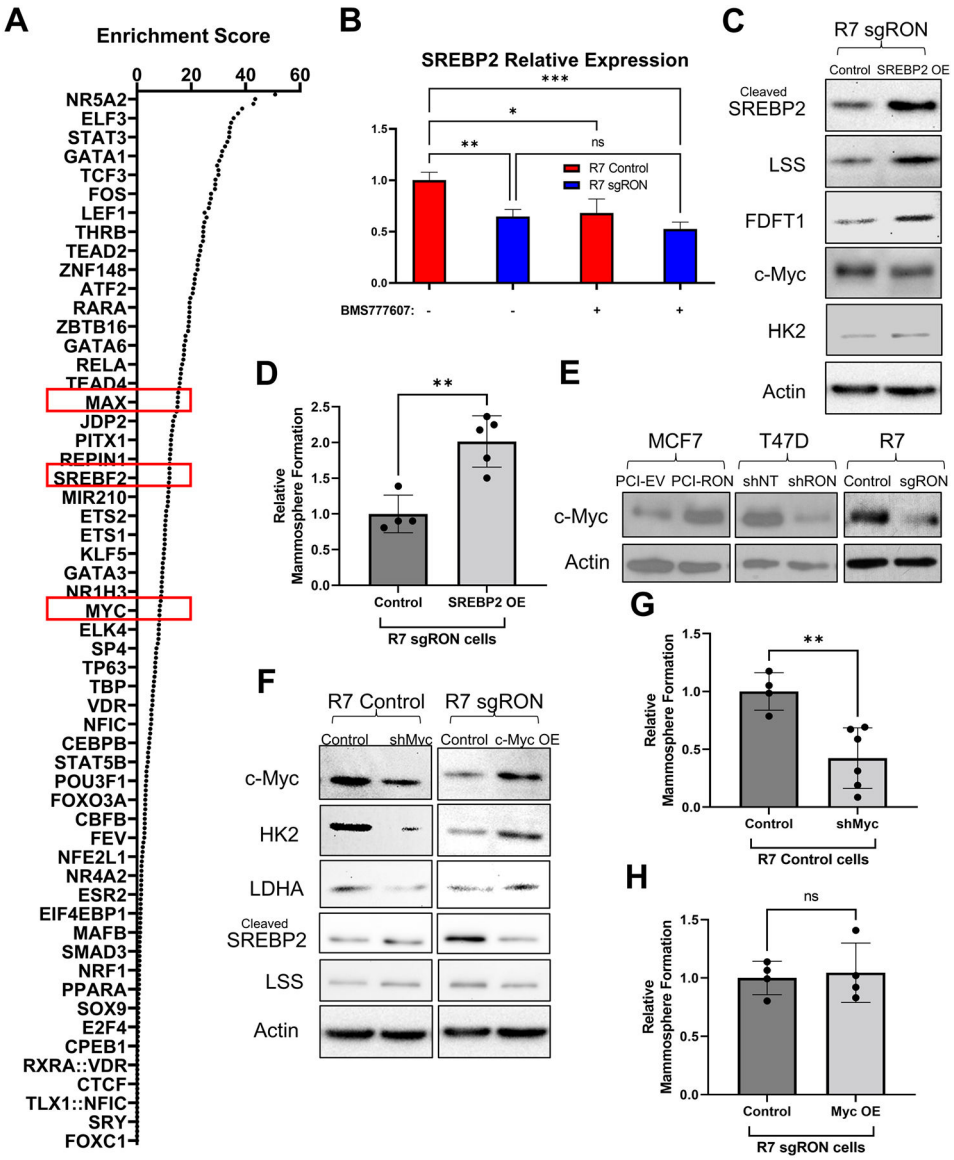

Figure 4. SREBP2 and c-Myc are required for RON-mediated upregulated of CBS and glycolysis, respectively.

(**A**) Enriched transcription factor signatures based on differentially expressed genes from RON-modulated T47D cells (Enrichr TRANSFAC); c-MYC/MAX and SREBF2 (SREBP2) are emphasized by red boxes. (**B**) Relative *SREBP2* gene expression determined by qRT-PCR analysis on samples from RON expressing R7 cells (R7 Control; n=3 biological replicates) versus isogenic RON-deplete counterparts (R7 sgRON; n=3 biological replicates) with and without RON inhibition through 5 μM BMS777607 treatment for 6 hours. (**C**) Western blot analysis of R7 sgRON cells with or without SREBP2 overexpression (SREBP2 OE) examining cleaved SREBP2 levels and CBS target gene levels (LSS, FDFT1), c-Myc, and glycolysis gene levels (HK2, LDHA) with actin used as a loading control. (**D**) Mammosphere formation of R7 sgRON cells with or without SREBP2 OE (n=3 biological replicates). (**E**) Western blot analysis of c-Myc expression in RON-modulated MCF7, T47D, and R7 cells with actin as a loading control. (**F**) Western blot analysis of R7 cells

with or without c-Myc knockdown by shRNA (shMyc) and R7 sgRON cells with c-Myc overexpression (c-Myc OE) examining c-Myc levels, glycolysis (HK2, LDHA), cleaved SREBP2, and CBS genes (FDFT1, LSS) with actin as a loading control. (**G**) Mammosphere formation of R7 cells with or without shMyc (n=3 biological replicates). (**H**) Mammosphere formation of R7 sgRON cells with or without c-Myc OE (n=3 biological replicates). Western blot expression comparisons are only intended to be made within individual boxes. Data displayed represent mean values ± SD. ns, not significant; *P<0.05; **P<0.01; ***P<0.001.

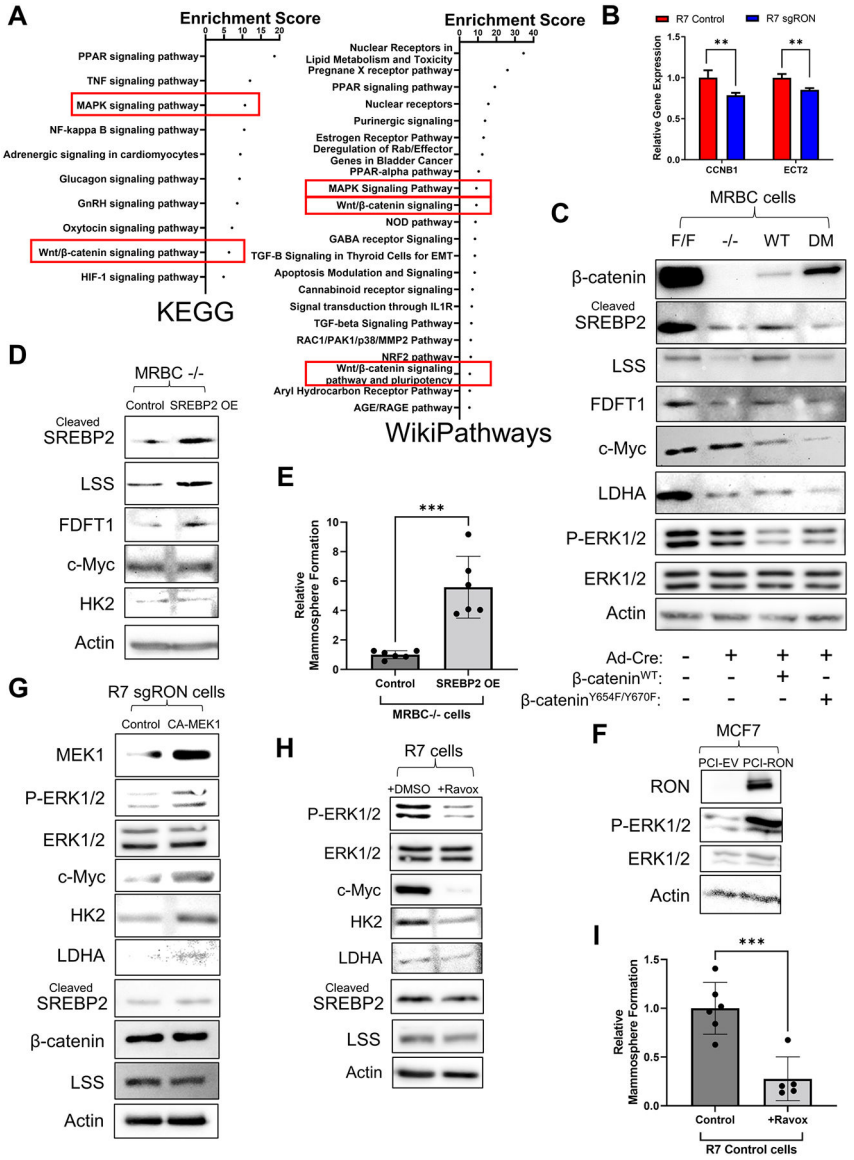

Figure 5. Non-canonical β-catenin activation is required for SREBP2 upregulation and ERK1/2 activation is required for c-Myc upregulation for respective CBS and glycolysis upregulation by RON in breast cancer cells.

(**A**) WikiPathways (2021) and KEGG (2021) pathway enrichment based on differentially expression genes from RON-modulated T47D cells (Enrichr); red boxes emphasize common hits that are known pathways activated by RON. (B) Relative gene expression of β-catenin target genes, *Ccnb1* and *Ect2*, determined by qRT-PCR analysis on samples from RON expressing R7 cells (R7 Control; n=3 biological replicates) versus isogenic RON-deplete counterparts (R7 sgRON; n=3 biological replicates) (C) Western blot analysis of samples from RON expressing MRBC cells with β-catenin modulation as noted examining cleaved (activated) SREBP2 levels, CBS enzyme levels (LSS, FDFT1), c-Myc levels, ERK1/2 activation (P-ERK1/2/Total ERK1/2) levels, and LDHA levels with actin as a loading control. (D) Western blot analysis of samples from MRBC −/− cells, lacking β-catenin, with and without SREBP2 overexpression (SREBP2 OE) examining SREBP2 levels, CBS

enzyme levels (LSS, FDFT1), c-Myc levels, and HK2 levels with actin as a loading control. (E) Mammosphere formation of MRBC −/− cells with and without SREBP2 OE (n=3 biological replicates). (F) Western blot analysis of samples from RON-modulated MCF7 cells examining ERK1/2 phosphorylation with total ERK1/2 and actin as a loading control. (G) Western blot analysis of R7 sgRON cells with and without expression of constitutively active MEK1 (CA-MEK1; an activator of ERK1/2) examining MEK1 levels, c-Myc levels, ERK1/2 activation (P-ERK1/2/Total ERK1/2) levels, LSS levels, cleaved SREBP2 levels, and β-catenin levels with actin as a loading control. (H) Western blot analysis of R7 cells with and without treatment of 20 μM Ravoxertinib (ERK1/2 inhibitor) for 4 hours examining c-Myc levels, ERK1/2 activation (P-ERK1/2/Total ERK1/2) levels, glycolysis enzyme (HK2, LDHA) levels, cleaved SREBP2 levels, and LSS levels with actin as a loading control. (I) Mammosphere formation of R7 cells with and without ERK1/2 inhibition (ERK*i*) via treatment with 20 μM Ravoxertinib (n=3 biological replicates). Western blot expression comparisons are only intended to be made within individual boxes. Data displayed represent mean values ± SD. **P<0.01; ***P<0.001.

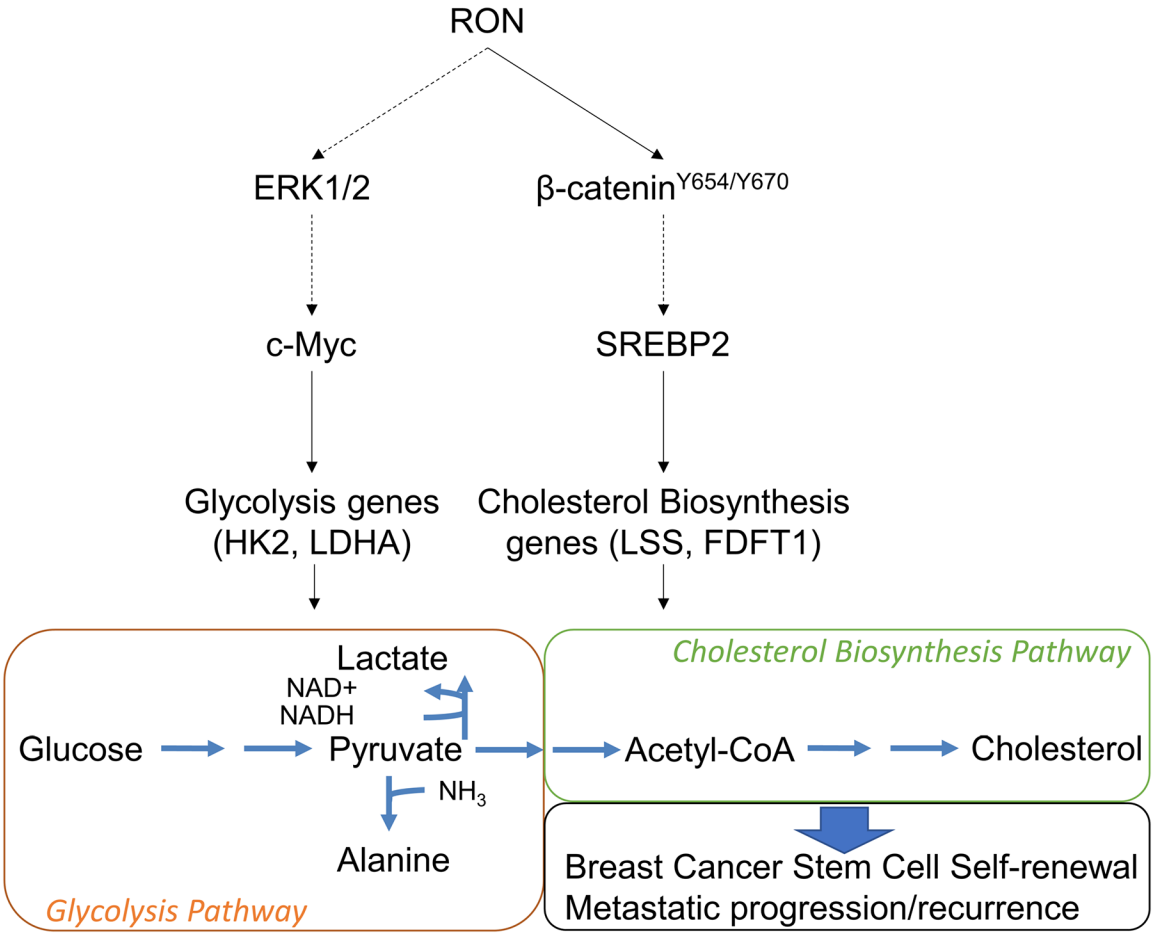

Figure 6. Working model depicting the role of RON in the promotion of breast cancer recurrence.

Diagram of the pathways and functional output of RON receptor expression in breast cancer cells. Our data show that RON dependent activation of c-Myc (through ERK1/2) and SREBP2 (through β-catenin) support glycolysis and cholesterol biosynthesis, respectively. Activation of these pathways by RON supports BCSC properties and breast cancer recurrence providing potential exciting new opportunities to target breast cancer progression in RON expressing tumors.